Pergamon

0045-7949(94)00635-0

Computers & Structures Vol. 57, No. 3, pp. 455–466, 1995
Elsevier Science Ltd
Printed in Great Britain
0045-7949/95 $9.50 + 0.00

TOTAL LAGRANGIAN FORMULATION FOR LAMINATED COMPOSITE PLATES ANALYSED BY THREE-DIMENSIONAL FINITE ELEMENTS WITH TWO-DIMENSIONAL KINEMATIC CONSTRAINTS

R. Zinno† and **E. J. Barbero**‡

†Department of Structural Engineering, University of Calabria, 87030 Arcavacata di Rende (CS), Italy

‡Department of Mechanical and Aerospace Engineering, West Virginia University, Morgantown, PO Box 6101, WV 26506, U.S.A.

(*Received* 18 *March* 1994)

Abstract—A three-dimensional element with two-dimensional kinematic constraints is developed for the geometric nonlinear analysis of laminated composite plates. The Newton–Raphson iterative method is adopted to trace the nonlinear equilibrium path. Maximum accuracy in the computation of stresses is achieved by postprocessing the stress results from constitutive equations with the aid of the equilibrium equations. Some numerical examples are presented to demonstrate the efficiency and the validity of the proposed element. A total Lagrangian description and the principle of virtual displacements is used to formulate the equilibrium equations.

1. INTRODUCTION

Fiber reinforced composite materials are being widely used in different branches of engineering because of their excellent mechanical properties [1]. These materials are formed by fibers of various kind (glass, steel, graphite, boron, etc.) surrounded by a matrix, usually a resin. Multidirectional (or laminated) composites are formed by several laminae, each containing a family of parallel fibers, but differently oriented from lamina to lamina.

One of the weakest links in laminated composites is the interlaminar strength and so the estimation of the interlaminar stresses is important in ensuring the integrity of the laminates. The single layer classical and shear deformation theories [2–4] based on a continuous displacement field through the thickness are adequate for predicting global response characteristics, such as maximum deflections and fundamental natural frequencies. The first-order and higher-order shear deformation theories yield improved global response over the classical laminate theory because the former account for transverse shear strains [5]. Both classical and refined plate theories based on a single continuous displacement field through the thickness give poor estimation of interlaminar stresses. The fact that some important modes of failure are related to the interlaminar stresses motivated research on refined theories that can model the layer-wise kinematics appropriately and predict interlaminar stresses accurately [6–10]. Unfortunately, the finite element implementation of these theories is not simple because they imply a large number of degrees of freedom per node. In a previous paper, Barbero [11] developed a new three-dimensional element for the linear analysis of multidirectional composite plates, using the formulation of Ahmad *et al.* [12] and applying the kinematic constraints of layer-wise constant shear theories (LCWS). The new element overcomes the problems linked with the two-dimensional LCWS theories, retains the precise calculation of stresses and has a physical interpretation of the degrees of freedom (DOF), the boundary conditions and stress resultants. This element [11] was validated by the patch test [13] and, for linear analysis, was extended to the analysis of general anisotropic shell-type structures [14].

The laminated composites are characterized by high values of strength/stiffness ratio and then they can be highly stressed and deformed to fully exploit the capability of these materials. Therefore, it is very important to consider change of configuration during deformation by geometrically nonlinear theories [15, 16]. The present study is an extension of the previous analyses, to include geometric nonlinearity, to develop its nonlinear finite element model and to investigate the effects of geometric nonlinearities on stresses and load–deflection behavior of laminated composite plates. To define the geometric nonlinear behavior, a total Lagrangian formulation is adopted, in which displacements are referred to the original configuration [17, 18]. The principle of virtual displacements is used to obtain the equilibrium equations.

To overcome the problem of the ill-conditioned equations shown by Ahmad *et al.* [12] and to reduce the number of the DOF, the assumption of incompressibility along the thickness is made. This assumption is quite valid for a broad class of problems of moderately thick multidirectional composites. A method is developed to apply the incompressibility using a constraint matrix, thus producing a symmetric, non-singular, banded global stiffness matrix.

The distribution of interlaminar stresses obtained directly by using the proposed element is layer-wise constant when the Von Kármán assumptions are made. Quadratic interlaminar stresses that satisfy the shear boundary conditions at the top and bottom surfaces of the plate are here obtained by postprocessing [19]. All components of stresses obtained at the Gauss integration points are extrapolated to the nodes using the procedure described by Cook [20].

Using the proposed element, it is possible to model problems with variable number of layers and variable thickness. Here some examples are presented to show the efficiency and the validity of the proposed element for nonlinear analysis.

2. FORMULATION

Let (x, y, z) be a stationary Cartesian coordinate system. Consider a laminated composite plate composed of n orthotropic laminae (Fig. 1). In each lamina the fibers are parallel and arbitrarily oriented with respect to the coordinate system. Assume that the plate can experience large displacements and rotations. We wish to analyse the equilibrium of the plate, taking into account the geometric nonlinearities.

In the Lagrangian description all variables are referred to a reference configuration, which can be the initial configuration or any other convenient configuration. The description in which all the variables are referred to the current configuration is called updated Lagrangian description and the one in which all variables are referred to the initial configuration is called total Lagrangian formulation, the latter one being used in this work. For the sake of completeness, the most important equations of this description are summarized below.

2.1. *Principle of virtual displacements*

The equilibrium of the plate is expressed using the principle of virtual work:

$$\int_{V_d} {}^{d}\tau_{ij}\,\delta\,{}_{d}e_{ij}\,\mathrm{d}V_d = \int_{V_d} {}^{d}f_i^{b}\,\delta u_i^{b}\,\mathrm{d}V_d + \int_{S_d} {}^{d}f_i^{s}\,\delta u_i^{s}\,\mathrm{d}S_d. \quad (1)$$

Here and in the following the left subscripts and superscripts on a quantity are used to indicate, respectively, the configuration in which the quantity occurs and the configuration in which the quantity is measured. In particular d indicates the deformed geometry and 0 the undeformed configuration.

In eqn (1):

${}^{d}\tau_{ij}$ are the Cartesian components of the Cauchy stress tensor on the deformed geometry;

${}_{d}e_{ij}$ are the Cartesian components of the infinitesimal strain tensor associated with the displacement from the undeformed to the deformed geometry;

${}^{d}f_i^{b}$ are the components of the externally applied body force vector;

${}^{d}f_i^{s}$ are the components of the externally surface force vector;

V_d is the volume measured on the deformed geometry;

S_d is the surface area measured on the deformed geometry;

δ indicates the variation, i.e.:

$$\delta\,{}_{d}e_{ij} = \delta\,\frac{1}{2}\left(\frac{\partial u_i}{\partial\,{}^{d}x_j} + \frac{\partial u_j}{\partial\,{}^{d}x_i}\right) = \frac{1}{2}\left(\frac{\partial \delta u_i}{\partial\,{}^{d}x_j} + \frac{\partial \delta u_j}{\partial\,{}^{d}x_i}\right); \quad (2)$$

where ${}^{d}x_i$ $(i = 1, 2, 3\;\; x_1 = x,\; x_2 = y, x_3 = z)$ are the Cartesian coordinates of a point in the deformed configuration and u_i $(i = 1, 2, 3\; u_1 = u,\; u_2 = v,\; u_3 = w)$ are the displacements from the undeformed to the deformed geometry $(u_i = {}^{d}x_i - {}^{0}x_i)$ and δu_i is the ith component of the virtual displacement.

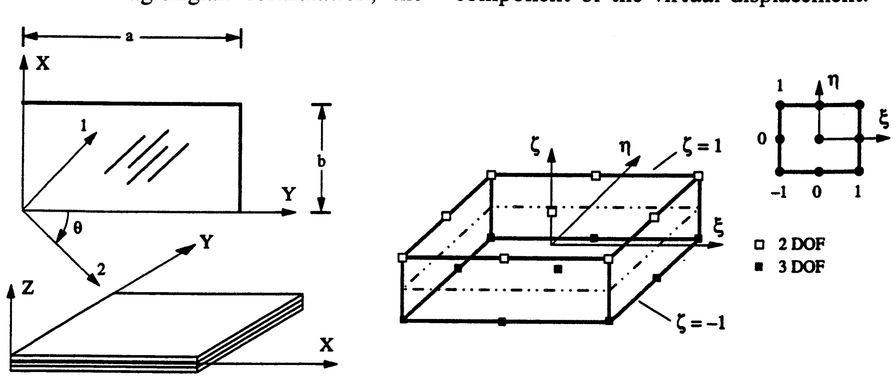

Fig. 1. Plate model, global and material coordinate systems.

this work. For the sake of
mportant equations of this
zed below.

lisplacements

plate is expressed using the
:

$f_i^b \delta u_i^b \, dV_d$

$$+ \int_{S_d} {}^d f_i^s \delta u_i^s \, dS_d. \quad (1)$$

wing the left subscripts and
ntity are used to indicate,
ration in which the quantity
tion in which the quantity is
r d indicates the deformed
leformed configuration.

components of the Cauchy
ormed geometry;
components of the infinitesi-
iated with the displacement
o the deformed geometry;
nts of the externally applied

nts of the externally surface

sured on the deformed geome-

a measured on the deformed

tion, i.e.:

$$\frac{\partial u_j}{\partial\, {}^d x_i}\Big) = \frac{1}{2}\left(\frac{\partial \delta u_i}{\partial\, {}^d x_j} + \frac{\partial \delta u_j}{\partial\, {}^d x_i}\right); \quad (2)$$

$x_1 = x,\ x_2 = y, x_3 = z)$ are the
of a point in the deformed
$= 1, 2, 3\ u_1 = u,\ u_2 = v,\ u_3 = w)$
from the undeformed to the
$_i = {}^d x_i - {}^0 x_i)$ and δu_i is the ith
ual displacement.

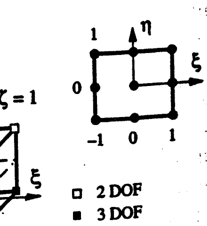

$\zeta = -1$

tems.

We remind that the Cauchy stress tensor is always referred to deformed configuration and is energetically conjugate to the infinitesimal strain tensor. Equation (1) can be solved directly if the deformed geometry is known. This is possible in linear analysis because we can assume that the deformed and undeformed geometry are coincident. In large deformation analysis this is not true. To express eqn (1) over a known configuration it is necessary to introduce the second Piola–Kirchhoff stress tensor and its energetically conjugate Green–Lagrange strain tensor.

2.2. *Total Lagrangian formulation*

A way to solve the geometrically nonlinear problem is to write an approximate solution referring all the variables to the undeformed geometry and linearizing the resulting equation. This equation can be solved iteratively using a suitable iterative method, such as Newton–Raphson, Riks, etc.

The left-hand side of eqn (1) can be transformed as [17, 18]:

$$\int_{V_d} {}^d\tau_{ij}\,\delta\, {}_d e_{ij}\, dV_d = \int_{V_0} {}^d_0 S_{ij}\,\delta\, {}^d_0\epsilon_{ij}\, dV_0; \quad (3)$$

where

${}^d_0 S_{ij}$ are the Cartesian components of the second Piola-Kirchhoff stress tensor;

${}^d_0\epsilon_{ij}$ are the Cartesian components of the Green-Lagrange strain tensor.

Both these quantities correspond to the deformed configuration, but are measured on the undeformed geometry. The components of the Green–Lagrange stress tensor are defined as

$${}^d_0\epsilon_{ij} = \tfrac{1}{2}({}_0u_{i,j} + {}_0u_{j,i} + {}_0u_{k,i}\,{}_0u_{k,j}), \quad (4)$$

where the left subscript on the differentiation indicates the following:

$${}_0u_{i,j} = \frac{\partial u_i}{\partial\, {}^0x_j}. \quad (5)$$

The right-hand side of eqn (1), becomes:

$$\int_{S_0} {}^d_0 f_i^s \delta u_i^s\, dS_0 + \int_{V_0} {}^d_0 f_i^b \delta u_i^b\, dV_0 = {}^dR; \quad (6)$$

where ${}^dR$ is the external virtual work.

To obtain the deformed geometry an iterative method must be adopted. With reference to the $(m+1)$th iteration we can write the following incremental decomposition of the stress tensor:

$${}^{m+1}_0 S_{ij} = {}^m_0 S_{ij} + {}_0S_{ij}. \quad (7)$$

and analogously for the strain tensor:

$${}^{m+1}_0\epsilon_{ij} = {}^m_0\epsilon_{ij} + {}_0\epsilon_{ij}. \quad (8)$$

The Green–Lagrange strain tensor ${}_0\epsilon_{ij}$ can be divided into its linear and nonlinear part as:

$${}_0\epsilon_{ij} = {}_0e_{ij} + {}_0\eta_{ij}; \quad (9)$$

where

$${}_0e_{ij} = \tfrac{1}{2}({}_0u_{i,j} + {}_0u_{j,i} + {}^m_0u_{k,i}\,{}_0u_{k,j} + {}_0u_{k,i}\,{}^m_0u_{k,j}); \quad (10)$$

$${}_0\eta_{ij} = \tfrac{1}{2}\,{}_0u_{k,i}\,{}_0u_{k,j}. \quad (11)$$

The equilibrium eqn (1) at the $(m+1)$th iteration, by using eqns (3)–(11) and noting that

$${}^d_0S_{ij} = {}_0C_{ijrs}\,{}^d_0\epsilon_{rs} \quad (12)$$

becomes (dropping the superscript d)

$$\int_{V_0} {}_0C_{ijrs}\,{}_0\epsilon_{rs}\,\delta\,{}_0\epsilon_{ij}\, dV_0 + \int_{V_0} {}^m_0S_{ij}\,\delta\,{}_0\eta_{ij}\, dV_0 = {}^{m+1}R - \int_{V_0} {}^m_0S_{ij}\,\delta\,{}_0e_{ij}\, dV_0; \quad (13)$$

where we used the relation $\delta\,{}^{m+1}_0\epsilon_{ij} = \delta\,{}_0\epsilon_{ij}$.

Equation (13) cannot be solved directly and then a linearization is needed by using the approximations (infinitesimal strain)

$${}_0S_{ij} = {}_0C_{ijrs}\,{}_0e_{rs}; \quad \delta\,{}_0\epsilon_{ij} = \delta\,{}_0e_{ij}, \quad (14)$$

obtaining the following approximate equilibrium equation:

$$\int_{V_0} {}_0C_{ijrs}\,{}_0e_{rs}\,\delta\,{}_0e_{ij}\, dV_0 + \int_{V_0} {}^m_0S_{ij}\,\delta\,{}_0\eta_{ij}\, dV_0 = {}^{m+1}R - \int_{V_0} {}^m_0S_{ij}\,\delta\,{}_0e_{ij}\, dV_0. \quad (15)$$

The right-hand side of eqn (15) represents the "out-of-balance virtual work" after the solution, produced by the previous linearizations. Using the Newton–Raphson iterative method the steps are repeated until the difference between the external and the internal virtual work is negligible within a certain convergence measure (here fixed at 1×10^{-3}).

3. FINITE ELEMENT DISCRETIZATION

3.1. *Three-dimensional elements*

Each layer of the plate is discretized by three-dimensional elements. The displacements can be written as follows:

$$\begin{Bmatrix} u \\ v \\ w \end{Bmatrix} = \sum_{i=1}^{N} \begin{bmatrix} N_i & 0 & 0 \\ 0 & N_i & 0 \\ 0 & 0 & N_i \end{bmatrix} \{\delta_i\}, \quad (16)$$

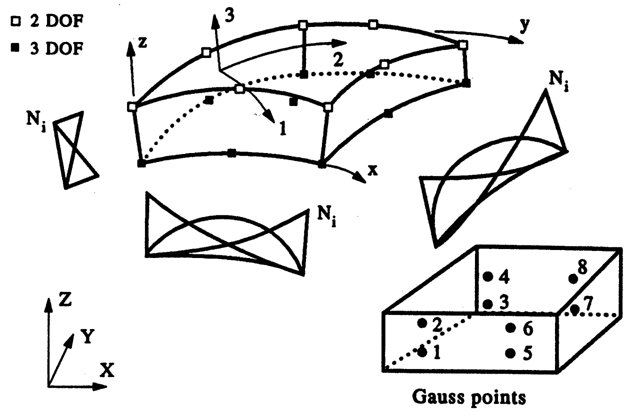

Fig. 2. Three-dimensional layer-wise element and its inter-polation functions.

where $\{\delta_i\} = \{u_i, v_i, w_i\}^{\mathrm{T}}$, N is the number of the nodes and $N_i = N_i(\xi, \eta, \zeta)$ are the interpolation functions equal for u, v and w. In the same way the coordinates of a point of the plate can be written as:

$$\begin{Bmatrix} x \\ y \\ z \end{Bmatrix} = \sum_{i=1}^{N} \begin{bmatrix} N_i & 0 & 0 \\ 0 & N_i & 0 \\ 0 & 0 & N_i \end{bmatrix} \{x_i\}, \tag{17}$$

where $\{x_i\} = \{x_i, y_i, z_i\}^{\mathrm{T}}$ are the nodal coordinate vectors (isoparametric elements).

The order of the interpolation functions N_i along the two coordinates of the surface of the plate can be chosen independently from the order through the thickness. Here quadratic interpolation functions are used for both (u, v) and (x, y), while linear variation is used in the thickness direction. The quadratic element has 18 nodes. Nodes 1–9 have 3 DOF (u, v, w), nodes 10–18 have 2 DOF (u, v), as shown in Fig. 2. The transverse deflection w is constant through the thickness.

The terms in eqn (15) can be rewritten as follows [18]:

$$\int_{V_0} {}_0C_{ijrs}\, {}_0e_{rs}\, \delta\, {}_0e_{ij}\, \mathrm{d}V_0 = \left(\int_{V_0} {}^{m}_{0}[\mathbf{B}_{\mathrm{L}}]^{\mathrm{T}}\, {}_0[\mathbf{C}]\, {}^{m}_{0}[\mathbf{B}_{\mathrm{L}}]\, \mathrm{d}V_0 \right) \{\delta\} = {}^{m}_{0}[\mathbf{K}_{\mathrm{L}}]\{\delta\}, \tag{18}$$

$$\int_{V_0} {}^{m}_{0}S_{ij}\, \delta\, {}_0\eta_{ij}\, \mathrm{d}V_0 = \left(\int_{V_0} {}^{m}_{0}[\mathbf{B}_{\mathrm{NL}}]^{\mathrm{T}}\, {}^{m}_{0}[\mathbf{S}]\, {}^{m}_{0}[\mathbf{B}_{\mathrm{NL}}]\, \mathrm{d}V_0 \right) \{\delta\} = {}^{m}_{0}[\mathbf{K}_{\mathrm{NL}}]\{\delta\}, \tag{19}$$

$$\int_{V_0} {}^{m}_{0}S_{ij}\, \delta\, {}_0e_{ij}\, \mathrm{d}V_0 = \int_{V_0} {}^{m}_{0}[\mathbf{B}_{\mathrm{L}}]^{\mathrm{T}}\, {}^{m}_{0}\{\bar{\mathbf{S}}\}\, \mathrm{d}V_0 = {}^{m}_{0}\{\mathbf{F}\}, \tag{20}$$

where

${}^{m}_{0}[\mathbf{B}_{\mathrm{L}}]$ is the linear strain–displacement transformation matrix;

${}^{m}_{0}[\mathbf{B}_{\mathrm{NL}}]$ is the nonlinear strain–displacement transformation matrix;

${}^{m}_{0}[\mathbf{S}]$ is the second Piola–Kirchhoff stress matrix.

${}^{m}_{0}\{\bar{\mathbf{S}}\}$ is the second Piola–Kirchhoff stress vector.

$\{\delta\}$ is the collection of the nodal $\{\delta_i\}$.

The order of ${}_0e^{\mathrm{T}}$ is $\{{}_0e_{xx}, {}_0e_{yy}, {}_0e_{zz}, 2{}_0e_{yz}, 2{}_0e_{xz}, 2{}_0e_{xy}\}$. The matrix ${}^{m}_{0}[\mathbf{B}_{\mathrm{L}}]$ can be divided into:

$${}^{m}_{0}[\mathbf{B}_{\mathrm{L}}] = {}^{m}_{0}[\mathbf{B}_{\mathrm{L0}}] + {}^{m}_{0}[\mathbf{B}_{\mathrm{L1}}], \tag{21}$$

where

$${}^{m}_{0}[\mathbf{B}_{\mathrm{L0}}] = \begin{bmatrix} {}_0N_{i,z} & 0 & 0 \\ 0 & {}_0N_{i,y} & 0 \\ 0 & 0 & 0 \\ 0 & {}_0N_{i,z} & {}_0N_{i,z} \\ {}_0N_{i,z} & 0 & N_{i,z} \\ {}_0N_{i,zy} & {}_0N_{i,z} & 0 \end{bmatrix} \tag{22}$$

and

$${}^{m}_{0}[\mathbf{B}_{\mathrm{L1}}] = \begin{bmatrix} {}^{m}_{0}u_{,x}\, {}_0N_{i,x} & {}^{m}_{0}v_{,x}\, {}_0N_{i,x} & {}^{m}_{0}w_{,x}\, {}_0N_{i,x} \\ {}^{m}_{0}u_{,y}\, {}_0N_{i,y} & {}^{m}_{0}v_{,y}\, {}_0N_{i,y} & {}^{m}_{0}w_{,y}\, {}_0N_{i,y} \\ 0 & 0 & 0 \\ {}^{m}_{0}u_{,y}\, {}_0N_{i,z} + {}^{m}_{0}u_{,z}\, {}_0N_{i,y} & {}^{m}_{0}v_{,y}\, {}_0N_{i,z} + {}^{m}_{0}v_{,z}\, {}_0N_{i,y} & {}^{m}_{0}w_{,y}\, {}_0N_{i,z} + {}^{m}_{0}w_{,z}\, {}_0N_{i,y} \\ {}^{m}_{0}u_{,x}\, {}_0N_{i,z} + {}^{m}_{0}u_{,z}\, {}_0N_{i,x} & {}^{m}_{0}v_{,x}\, {}_0N_{i,z} + {}^{m}_{0}v_{,z}\, {}_0N_{i,x} & {}^{m}_{0}w_{,x}\, {}_0N_{i,z} + {}^{m}_{0}w_{,z}\, {}_0N_{i,x} \\ {}^{m}_{0}u_{,x}\, {}_0N_{i,y} + {}^{m}_{0}u_{,y}\, {}_0N_{i,x} & {}^{m}_{0}v_{,x}\, {}_0N_{i,y} + {}^{m}_{0}v_{,y}\, {}_0N_{i,x} & {}^{m}_{0}w_{,x}\, {}_0N_{i,y} + {}^{m}_{0}w_{,y}\, {}_0N_{i,x} \end{bmatrix}. \tag{23}$$

In eqns (22) and (23) the third row represents the incompressibility condition ($_0e_{zz}=0$) that is an assumption valid for a broad class of problems of moderately thick laminated plates. The derivatives of the displacements with respect to the global axes (x, y, z) are obtained in the standard way as:

$$\begin{bmatrix} {}^m_0u_{,x} & {}^m_0v_{,x} & {}^m_0w_{,x} \\ {}^m_0u_{,y} & {}^m_0v_{,y} & {}^m_0w_{,y} \\ {}^m_0u_{,z} & {}^m_0v_{,z} & {}^m_0w_{,z} \end{bmatrix} = {}^0[\mathbf{J}]^{-1} \begin{bmatrix} {}^mu_{,\xi} & {}^mv_{,\xi} & {}^mw_{,\xi} \\ {}^mu_{,\eta} & {}^mv_{,\eta} & {}^mw_{,\eta} \\ {}^mu_{,\zeta} & {}^mv_{,\zeta} & {}^mw_{,\zeta} \end{bmatrix}, \quad (24)$$

where the Jacobian matrix is defined as

$${}^0[\mathbf{J}] = \begin{bmatrix} {}^0x_{,\xi} & {}^0y_{,\xi} & {}^0z_{,\xi} \\ {}^0x_{,\eta} & {}^0y_{,\eta} & {}^0z_{,\eta} \\ {}^0x_{,\zeta} & {}^0y_{,\zeta} & {}^0z_{,\zeta} \end{bmatrix}. \quad (25)$$

The nonlinear strain–displacement matrix ${}^m_0[\mathbf{B}_{\mathrm{NL}}]$ is

$${}^m_0[\mathbf{B}_{\mathrm{NL}}] = \begin{bmatrix} {}^m_0[\bar{\mathbf{B}}_{\mathrm{NL}}] & \{\bar{0}\} & \{\bar{0}\} \\ \{\bar{0}\} & {}^m_0[\bar{\mathbf{B}}_{\mathrm{NL}}] & \{\bar{0}\} \\ \{\bar{0}\} & \{\bar{0}\} & {}^m_0[\bar{\mathbf{B}}_{\mathrm{NL}}] \end{bmatrix} \quad (26)$$

where

$${}^m_0[\bar{\mathbf{B}}_{\mathrm{NL}}] = \begin{bmatrix} {}_0N_{1,x} & 0 & 0 & {}_0N_{2,x} & \cdots & {}_0N_{N,x} \\ {}_0N_{1,y} & 0 & 0 & {}_0N_{2,y} & \cdots & {}_0N_{N,y} \\ {}_0N_{1,z} & 0 & 0 & {}_0N_{2,z} & \cdots & {}_0N_{N,z} \end{bmatrix}$$

and

$$\{\bar{0}\} = \begin{Bmatrix} 0 \\ 0 \\ 0 \end{Bmatrix}. \quad (27)$$

$$\begin{Bmatrix} {}_0S^k_{11} \\ {}_0S^k_{22} \\ {}_0S^k_{33} \\ {}_0S^k_{23} \\ {}_0S^k_{13} \\ {}_0S^k_{12} \end{Bmatrix} = \begin{bmatrix} {}_0C^k_{11} & {}_0C^k_{12} & {}_0C^k_{13} & 0 & 0 & 0 \\ {}_0C^k_{12} & {}_0C^k_{22} & {}_0C^k_{23} & 0 & 0 & 0 \\ {}_0C^k_{13} & {}_0C^k_{23} & {}_0C^k_{33} & 0 & 0 & 0 \\ 0 & 0 & 0 & {}_0C^k_{44} & 0 & 0 \\ 0 & 0 & 0 & 0 & {}_0C^k_{55} & 0 \\ 0 & 0 & 0 & 0 & 0 & {}_0C^k_{66} \end{bmatrix} \begin{Bmatrix} {}_0\epsilon^k_{11} \\ {}_0\epsilon^k_{22} \\ {}_0\epsilon^k_{33} \\ 2{}_0\epsilon^k_{23} \\ 2{}_0\epsilon^k_{13} \\ 2{}_0\epsilon^k_{12} \end{Bmatrix}. \quad (31)$$

The second Piola–Kirchhoff stress matrix is defined as

$${}^m_0[\mathbf{S}] = \begin{bmatrix} {}^m_0[\tilde{\mathbf{S}}] & [\bar{0}] & [\bar{0}] \\ [\bar{0}] & {}^m_0[\tilde{\mathbf{S}}] & [\bar{0}] \\ [\bar{0}] & [\bar{0}] & {}^m_0[\tilde{\mathbf{S}}] \end{bmatrix}, \quad (28)$$

where

$${}^m_0[\tilde{\mathbf{S}}] = \begin{bmatrix} {}^m_0S_{xx} & {}^m_0S_{xy} & {}^m_0S_{xz} \\ {}^m_0S_{yx} & {}^m_0S_{yy} & {}^m_0S_{yz} \\ {}^m_0S_{zx} & {}^m_0S_{zy} & {}^m_0S_{zz} \end{bmatrix}$$

and

$$[\bar{0}] = \begin{bmatrix} 0 & 0 & 0 \\ 0 & 0 & 0 \\ 0 & 0 & 0 \end{bmatrix}. \quad (29)$$

The second Piola–Kirchhoff stress vector is

$${}^m_0\{\hat{\mathbf{S}}\} = \{{}^m_0S_{xx}, {}^m_0S_{yy}, {}^m_0S_{zz}, {}^m_0S_{yz}, {}^m_0S_{xz}, {}^m_0S_{xy}\}^{\mathrm{T}}. \quad (30)$$

In eqns (29) and (30), ${}^m_0S_{zz}$ is replaced by zero and the other stress components are obtained by the constitutive relation (31)–(38) because of the incompressibility conditions and of the assumptions introduced in the following section.

3.2. *Constitutive equations*

For each layer, the second Piola–Kirchhoff stress tensor components ($_0S_{ij}$) and the Green–Lagrange strain tensor components ($_0\epsilon_{ij}$) are related by eqn (12) and approximated by eqn (14). Equation (12) can be written for each layer in the multidirectional composite plate. Using the property ${}_0S^k_{ij} = {}_0S^k_{ji}$ and reordering the terms of the $_0[\mathbf{S}]$ and $_0[\epsilon]$ as vectors, for each layer in the plate, we can rewrite eqn (12) with respect to the material directions (1, 2, 3) as follows [21]:

For a large range of problems we can suppose that the axial deformation of segments normal to the middle surface is zero during the deformation. Then we have that ${}_0\epsilon^k_{33}=0$ and the normal stress ${}_0S^k_{33}$ is negligible (${}_0S^k_{33}=0$).

Therefore we can write the strain–stress relation for an orthotropic layer using the compliance matrix ${}_0[R^k_{ij}]$ as follows:

$$\begin{Bmatrix} {}_0\epsilon^k_{11} \\ {}_0\epsilon^k_{22} \\ 0 \\ 2{}_0\epsilon^k_{23} \\ 2{}_0\epsilon^k_{13} \\ 2{}_0\epsilon^k_{12} \end{Bmatrix} = \begin{bmatrix} {}_0R^k_{11} & {}_0R^k_{12} & 0 & 0 & 0 & 0 \\ {}_0R^k_{12} & {}_0R^k_{22} & 0 & 0 & 0 & 0 \\ 0 & 0 & 0 & 0 & 0 & 0 \\ 0 & 0 & 0 & {}_0R^k_{44} & 0 & 0 \\ 0 & 0 & 0 & 0 & {}_0R^k_{55} & 0 \\ 0 & 0 & 0 & 0 & 0 & {}_0R^k_{66} \end{bmatrix} \begin{Bmatrix} {}_0S^k_{11} \\ {}_0S^k_{22} \\ 0 \\ {}_0S^k_{23} \\ {}_0S^k_{13} \\ {}_0S^k_{12} \end{Bmatrix}, \quad (32)$$

where the third row and column are deleted for the previous assumptions.

The terms of $[R]$ can be written in terms of engineering constants:

$$ {}_0R_{11}=\frac{1}{E_1^k};\quad {}_0R_{12}^k=-\frac{\nu_{21}^k}{E_2^k};\quad {}_0R_{22}^k=\frac{1}{E_2^k}; $$

$$ {}_0R_{44}=\frac{1}{G_{23}^k};\quad {}_0R_{55}^k=\frac{1}{G_{13}^k};\quad {}_0R_{66}^k=\frac{1}{G_{12}^k}. \qquad (33) $$

The statement that the normals remain perpendicular to the middle surface after deformation has been deliberately omitted. This omission allows the plate to experience shear deformations. Moreover, if we use one element for each lamina (or cluster of laminae) we will omit the statement that the normals remain practically straight after deformation, obtaining the layer-wise model, where the rotation of each lamina can be different from the other ones.

Using the rotation matrix $[\mathbf{T}^k]$:

$$ [\mathbf{T}^k]=\begin{bmatrix} \cos^2\vartheta^k & \sin^2\vartheta^k & 0 & 0 & 0 & 2\sin\vartheta^k\cos\vartheta^k \\ \sin^2\vartheta^k & \cos^2\vartheta^k & 0 & 0 & 0 & -2\sin\vartheta^k\cos\vartheta^k \\ 0 & 0 & 1 & 0 & 0 & 0 \\ 0 & 0 & 0 & \cos\vartheta^k & -\sin\vartheta^k & 0 \\ 0 & 0 & 0 & \sin\vartheta^k & \cos\vartheta^k & 0 \\ -\sin\vartheta^k\cos\vartheta^k & \sin\vartheta^k\cos\vartheta^k & 0 & 0 & 0 & \cos^2\vartheta^k-\sin^2\vartheta^k \end{bmatrix}, \qquad (34) $$

Inverting the expression (32) we obtain:

$$ {}_0[\mathbf{C}_{123}^k]=\begin{bmatrix} Q_{11}^k & {}_0Q_{12}^k & 0 & 0 & 0 & 0 \\ {}_0Q_{12}^k & {}_0Q_{22}^k & 0 & 0 & 0 & 0 \\ 0 & 0 & 0 & 0 & 0 & 0 \\ 0 & 0 & 0 & k^2\,{}_0C_{44}^k & 0 & 0 \\ 0 & 0 & 0 & 0 & k^2\,{}_0C_{55}^k & 0 \\ 0 & 0 & 0 & 0 & 0 & {}_0Q_{66}^k \end{bmatrix}. \qquad (34) $$

The coefficients of $[\mathbf{C}_{123}]^k$ can be written in function of the engineering constants as

$$ {}_0Q_{11}^k=\frac{E_1^k}{1-\nu_{12}^k\nu_{21}^k}; $$

$$ {}_0Q_{12}^k=\frac{\nu_{12}^kE_2^k}{1-\nu_{12}^k\nu_{21}^k}=\frac{\nu_{21}^kE_1^k}{1-\nu_{12}^k\nu_{21}^k}; $$

$$ {}_0Q_{22}^k=\frac{E_2^k}{1-\nu_{12}^k\nu_{21}^k};\quad {}_0C_{44}^k=Q_{44}^k=G_{23}^k; $$

$$ {}_0Q_{55}^k=Q_{55}^k=G_{13}^k;\quad {}_0Q_{66}^k=G_{12}^k; \qquad (35) $$

where E_1^k, E_2^k are the Young's moduli along the directions 1, 2; G_{23}^k, G_{13}^k, G_{12}^k are the shear moduli and ν_{12}^k and ν_{21}^k are the Poisson's coefficients, respectively.

The shear correction coefficient k is included as required by FSDT ($k^2=5/6$) [11]. Using this expression for ${}_0[\mathbf{C}_{123}]$ and fixing for ${}_0\epsilon_{33}^k$ the value zero, we can overcome large stiffness coefficients for relative displacements along an edge corresponding to the plate thickness and then overcome the numerical problem that can produce ill-conditioned equations when the shell thickness becomes small compared to the other dimensions in the element.

we can obtain the expression of ${}_0[\mathbf{C}_{xyz}^k]$ written with respect to the global system of reference:

$$ {}_0[\mathbf{C}_{xyz}^k]=[\mathbf{T}^k]\,{}_0[\mathbf{C}_{123}^k][\mathbf{T}^k]^{-1}. \qquad (37) $$

Thus the relationship between stresses and strains with reference to the global coordinate system, becomes:

$$ {}_0\{\mathbf{S}\}={}_0[\mathbf{C}_{xyz}]_0\{\epsilon\}. \qquad (38) $$

3.3. *Application of the incompressibility constraint*

The incompressibility condition (${}_0\epsilon_{zz}=0$) represented by eqns (22) and (23) leads to a unique transverse deflection w on each vertical to the mid-plane of the plate (Fig. 3).

The stiffness matrices ${}_0^m[\mathbf{K}_L]$ and ${}_0^m[\mathbf{K}_{NL}]$ are obtained performing the integrations (18) and (19) as a standard 18-node element with 3 DOF per node, where the interpolation functions N_s in eqns (16) and (17) follow the considerations previously described. The global stiffness matrix obtained from the previous matrices is singular because w is constant through the thickness. Therefore it is necessary to reduce all the w-DOF on each vertical to a single DOF.

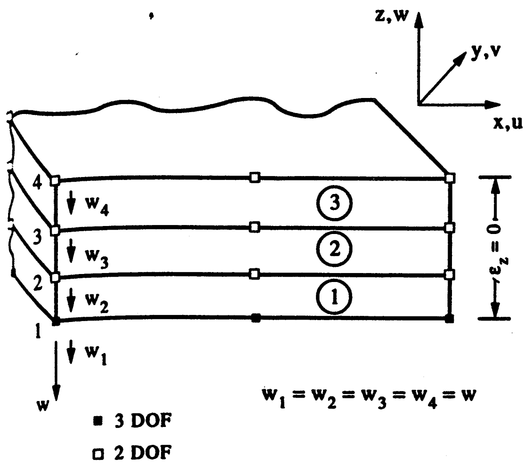

Fig. 3. Incompressibility condition and position of the master nodes.

At element level we choose the master nodes at the bottom of the element as displayed in Fig. 3. Making this choice, it is possible to divide the nodal displacement vector into two parts. The first $\{\delta^1\}$ collects the independent DOF (u and v of all the nodes and w of the master nodes), while the second $\{\delta^2\}$ collects the remaining dependent nodal displacements. The condition of incompressibility can be introduced as constraint equations using a suitable matrix [**A**] as follows [22]:

$$\{\delta\} = \begin{Bmatrix} \{\delta^1\} \\ \{\delta^2\} \end{Bmatrix} = [\mathbf{A}]\{\delta^1\}. \tag{39}$$

The dimensions of the matrix [**A**] are 54×45 because all the DOF of the 18 nodes into each element have to be connected to 45 independent DOF. The constraint matrix [**A**] is constructed as

$$\begin{Bmatrix} u_1 \\ v_1 \\ w_1 \\ \cdot \\ \cdot \\ \cdot \\ u_9 \\ v_9 \\ w_9 \\ \cdot \\ \cdot \\ \cdot \\ u_{18} \\ v_{18} \\ w_{18} \end{Bmatrix} = \begin{bmatrix} 1 & 0 & \cdots & 0 & 0 & \cdots & 0 & 0 & 0 & \cdots & 0 \\ 0 & 1 & \cdots & 0 & 0 & \cdots & 0 & 0 & 0 & \cdots & 0 \\ 0 & 0 & \cdots & 0 & 0 & \cdots & 0 & 0 & 1 & \cdots & 0 \\ \cdot & \cdot & \cdots & \cdot & \cdot & \cdots & \cdot & \cdot & \cdot & \cdots & \cdot \\ \cdot & \cdot & \cdots & \cdot & \cdot & \cdots & \cdot & \cdot & \cdot & \cdots & \cdot \\ \cdot & \cdot & \cdots & \cdot & \cdot & \cdots & \cdot & \cdot & \cdot & \cdots & \cdot \\ 0 & 0 & \cdots & 1 & 0 & \cdots & 0 & 0 & 0 & \cdots & 0 \\ 0 & 0 & \cdots & 0 & 1 & \cdots & 0 & 0 & 0 & \cdots & 0 \\ 0 & 0 & \cdots & 0 & 0 & \cdots & 0 & 0 & 0 & \cdots & 1 \\ \cdot & \cdot & \cdots & \cdot & \cdot & \cdots & \cdot & \cdot & \cdot & \cdots & \cdot \\ \cdot & \cdot & \cdots & \cdot & \cdot & \cdots & \cdot & \cdot & \cdot & \cdots & \cdot \\ \cdot & \cdot & \cdots & \cdot & \cdot & \cdots & \cdot & \cdot & \cdot & \cdots & \cdot \\ 0 & 0 & \cdots & 0 & 0 & \cdots & 1 & 0 & 0 & \cdots & 0 \\ 0 & 0 & \cdots & 0 & 0 & \cdots & 0 & 1 & 0 & \cdots & 0 \\ 0 & 0 & \cdots & 0 & 0 & \cdots & 0 & 0 & 0 & \cdots & 1 \end{bmatrix} \begin{Bmatrix} u_1 \\ v_1 \\ \cdot \\ \cdot \\ u_9 \\ v_9 \\ \cdot \\ \cdot \\ \cdot \\ u_{18} \\ v_{18} \\ w_1 \\ \cdot \\ \cdot \\ \cdot \\ w_9 \end{Bmatrix}. \tag{40}$$

At element level we have, from eqns (15), (18), (19) and (20):

$$[{}_0^m[\bar{\mathbf{K}}_L] + {}_0^m[\bar{\mathbf{K}}_{NL}]]\begin{Bmatrix} \{\delta^1\} \\ \{\delta^2\} \end{Bmatrix} = \{{}^{m+1}\{\bar{\mathbf{R}}\} - {}_0^m\{\bar{\mathbf{F}}\}\}. \tag{41}$$

The overlines indicate that the two matrices ${}_0^m[\bar{\mathbf{K}}_L]$ and ${}_0^m[\bar{\mathbf{K}}_{NL}]$ are reordered, interchanging the rows and the columns of the original ${}_0^m[\mathbf{K}_L]$ and ${}_0^m[\mathbf{K}_{NL}]$ to follow the new order in $\{\delta\}$. The vectors on the right hand side of eqn (41) also have to be reordered following the new order of $\{\delta\}$.

Using the transformation (39), it is possible to write:

$$[{}_0^m[\bar{\mathbf{K}}_L] + {}_0^m[\bar{\mathbf{K}}_{NL}]][\mathbf{A}]\{\delta^1\} = \{{}_0^{m+1}\{\bar{\mathbf{R}}\} - {}_0^m\{\bar{\mathbf{F}}\}\}. \tag{42}$$

To obtain a symmetric coefficient matrix, we premultiply both sides of eqn (42) with $[\mathbf{A}]^T$:

$$[\mathbf{A}]^T[{}_0^m[\bar{\mathbf{K}}_L] + {}_0^m[\bar{\mathbf{K}}_{NL}]][\mathbf{A}]\{\delta^1\} = [\mathbf{A}]^T\{{}^{m+1}\{\bar{\mathbf{R}}\} - {}_0^m\{\bar{\mathbf{F}}\}\}, \tag{43}$$

or

$$[{}_0^m[\tilde{\mathbf{K}}_L] + {}_0^m[\tilde{\mathbf{K}}_{NL}]]\{\delta^1\} = \{{}^{m+1}\{\tilde{\mathbf{R}}\} - {}_0^m\{\tilde{\mathbf{F}}\}\}, \tag{44}$$

where the element stiffness matrix has now the dimensions 45×45 and the "out of balance virtual work" vector has 45 independent components.

If more than one layer is present in the laminate, another condensation procedure must be done for each vertical connecting all the w-displacements to only one master node (e.g. w-master node at the bottom of the laminate). This has been easily achieved through the usual element assembly procedure by assigning the same global node number of the master node to all the w-DOF located on its normal [11, 13].

4. REFINED COMPUTATION OF THE STRESS

Using the constitutive eqns (12) and (14), it is possible to calculate the stresses at the Gauss points from the displacement field solution of the problem. These stresses can be easily extrapolated to the nodes by the procedure explained in Ref. [20]. The distribution of ${}^d_0S_x$, ${}^d_0S_y$ and ${}^d_0S_{xy}$ is linear through the thickness while ${}^d_0S_{xz}$ and ${}^d_0S_{yz}$ are layer-wise linear if the full Green–Lagrange strain tensor is adopted and layer-wise constant if the Von Kármán approximations are made. Selective reduced integration is used on the shear-related terms.

Quadratic interlaminar shear stresses that satisfy the boundary conditions at the top and at the bottom surfaces of the plate are obtained in this work for laminated plates modeled with three-dimensional-layer-wise (3DLW) elements. A procedure to obtain an approximation of the shear distribution through each layer with quadratic functions was proposed in Ref. [19]. All the details about the method developed for the linear analysis of plates can be found in Refs [8, 11, 13]. Here we point out the procedure in nonlinear analysis adopted to calculate the jumps in ${}^d_0S_{xz,z}$ and ${}^d_0S_{yz,z}$ at each interface using the following equilibrium equations:

$$\frac{\partial\, {}^d_0S_{xz}}{\partial\, {}^0z} = -\left(\frac{\partial\, {}^d_0S_x}{\partial\, {}^0x} + \frac{\partial\, {}^d_0S_{xy}}{\partial\, {}^0y}\right);$$

$$\frac{\partial\, {}^d_0S_{yz}}{\partial\, {}^0z} = -\left(\frac{\partial\, {}^d_0S_{xy}}{\partial\, {}^0x} + \frac{\partial\, {}^d_0S_y}{\partial\, {}^0y}\right). \qquad (45)$$

To use the method proposed in Ref. [19] the shear stresses ${}^d_0S_{yz}$ and ${}^d_0S_{xz}$ must be constant through the layer thickness. Thus, to obtain the refined computations of the shear stresses, the Von Kármán assumptions are made (see also Sections 5 and 6).

The computation of the second derivatives of the interpolation functions with respect to the global coordinate was explained in detail in Refs [8, 11, 13, 14]. The derivatives of the second Piola–Kirchhoff stress tensor components with respect to ${}^0x$ and ${}^0y$ can be obtained from the constitutive eqns (38) using the derivatives with respect to ${}^0x$ and ${}^0y$ of the Green–Lagrange strain tensor components:

$${}^d_0\{\bar{\mathbf{S}}\}_{,z} = {}_0[\mathbf{C}_{xyz}]\,{}^d_0\{e\}_{,z};$$

$${}^d_0\{\bar{\mathbf{S}}\}_{,y} = {}_0[\mathbf{C}_{xyz}]\,{}^d_0\{e\}_{,y}. \qquad (4$$

The derivatives of the Green–Lagrange strain tensor components, applying the Von Kármán assumptions appear as:

$${}^d_0\epsilon_{xx,x} = \frac{\partial^2 u}{\partial\, {}^0x^2} + \frac{\partial^2 w}{\partial\, {}^0x^2}\frac{\partial w}{\partial^0 x}, \qquad (4$$

$$2\,{}^d_0\epsilon_{xy,x} = \frac{\partial^2 u}{\partial\, {}^0x\,\partial\, {}^0y} + \frac{\partial^2 v}{\partial\, {}^0x^2} + \frac{\partial^2 w}{\partial\, {}^0x^2}\frac{\partial w}{\partial\, {}^0y} + \frac{\partial^2 w}{\partial\, {}^0x\,\partial\, {}^0y}\frac{\partial w}{\partial\, {}^0x}, \qquad (48$$

with the other components obtained by suitable permutations. In particular the derivatives of ${}^d_0\epsilon_{zz}$ are equal to zero.

Using the first and second-order derivatives of the interpolation functions, it is possible to calculate the second-order derivatives of the nodal displacements and by the previous eqns (45) reach the values of the jumps needed to trace the parabolic distributions of the shear stresses.

5. VON KÁRMÁN PLATE THEORY

The previous relationships are formulated in a general way to be useful for the extension to shell analysis. However, for the analysis of composite laminated plate the Von Kármán theory can be adopted to approximate the Green–Lagrange strain tensor. In fact when the transverse deflection is not small (but comparable to the thickness of the plate) and inplane displacement gradients are small, it is possible to assume that the products and squares of the slopes of inplane displacements are small compared to unity and can be neglected.

The Green–Lagrange strain tensor reduces to:

$${}^d_0\epsilon_{xx} = u_{,x} + \tfrac{1}{2}(w_{,x})^2;\quad {}^d_0\epsilon_{yy} = v_{,y} + \tfrac{1}{2}(w_{,y})^2;$$

$${}^d_0\epsilon_{zz} = 0;\quad 2\,{}^d_0\epsilon_{yz} = v_{,z} + w_{,y};$$

$$2\,{}^d_0\epsilon_{xz} = u_{,z} + w_{,x};$$

$$2\,{}^d_0\epsilon_{xy} = u_{,y} + v_{,x} + w_{,x}w_{,y}. \qquad (49$$

The incompressibility condition leads to $w_{,z} = 0$ and ${}^d_0\epsilon_{zz} = 0$.

Table 1. Material properties

Material I (isotropic): $E = 20{,}000\ \mathrm{N\,mm^{-2}}$; $\nu = 0.3$;
Material II: $E_1 = 25.0 \times 10^4\ \mathrm{N\,mm^{-2}}$; $E_2 = 2.0 \times 10^4\ \mathrm{N\,mm^{-2}}$ $G_{23} = 4 \times 10^3\ \mathrm{N\,mm^{-2}}$; $G_{12} = G_{13} = 1.0 \times 10^4\ \mathrm{N\,mm^{-2}}$; $\nu_{12} = 0.25$.

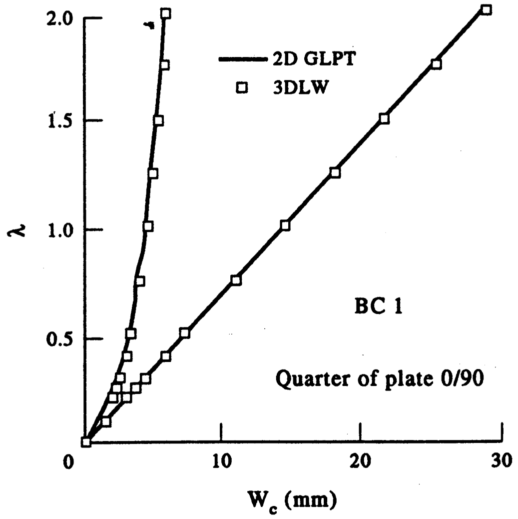

Fig. 6. Simply supported square cross-ply plate: linear and nonlinear central deflections.

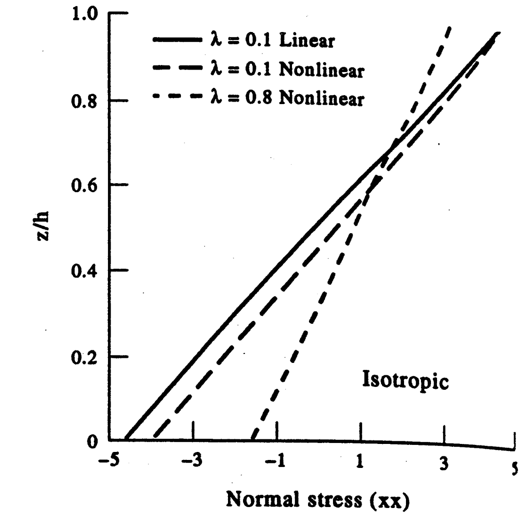

Fig. 8. Isotropic square plate: through the thickness normal stress distribution.

2D-GLPT results and the 3DLW ones, we consider a $4 \times 4 \times 2$ mesh to model a simply supported angle-ply plate subjected to a uniformly distributed transverse load, as in the previous examples.

The material properties are the same as in the previous example. The boundary conditions necessary to obtain the 2D-GLPT solution are the following (BC3):

$$v_0 = w_0 = \psi_x = 0 \quad \text{at } y = \pm a/2;$$

$$u_0 = w_0 = \psi_y = 0 \quad \text{at } x = \pm a/2.$$

These boundary conditions cannot be modeled with the 3DLW elements because fixing $u = 0$ through the thickness, for example, will automatically fix to zero the rotations along x (or around y) that are the ψ_x in the 2D-GLPT model. Observing Fig. 7, it is clear that the 2D-GLPT solution obtained with the BC3 boundary conditions is between the 3DLW results obtained using the BC1 and the BC2 conditions. In particular, with the BC2 conditions we have a plate practically clamped, obtaining the stiffest structure. In the linear case the two-dimensional solution appears the less stiff.

6.2. *Stresses distribution*

6.2.1. *Normal stress* S_{xz} *for a clamped isotropic plate*. Figure 8 shows the variation of S_{xz}/p through the thickness of the isotropic plate described in Section 6.1.1. The stresses are measured in the Gauss point with coordinates $x = 0.44717a$, $y = 0.052831a$ and are adimensionalized with the relation $(S_{xx}/p) \times 10^{-4}$.

The effect of the nonlinearities is to reduce the value of the stress at the top and bottom surfaces and to increase it at the middle surface of the plate.

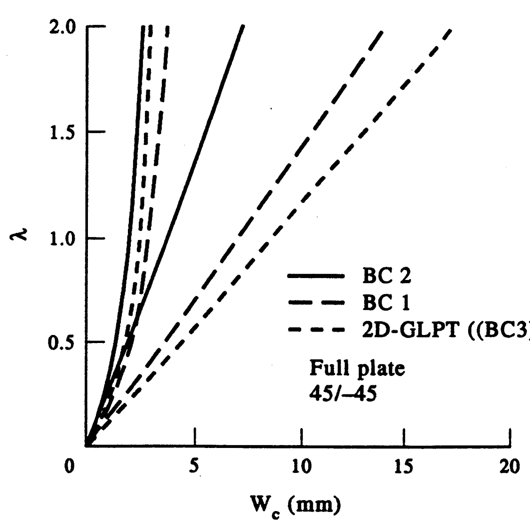

Fig. 7. Simply supported square angle-ply plate: linear and nonlinear central deflections.

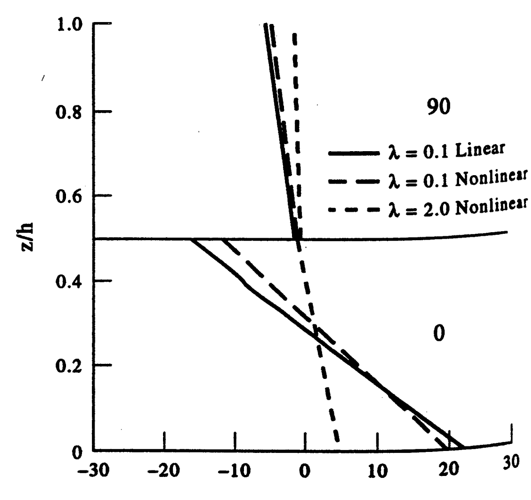

Fig. 9. Simply supported square cross-ply plate: through the thickness normal stress distribution.

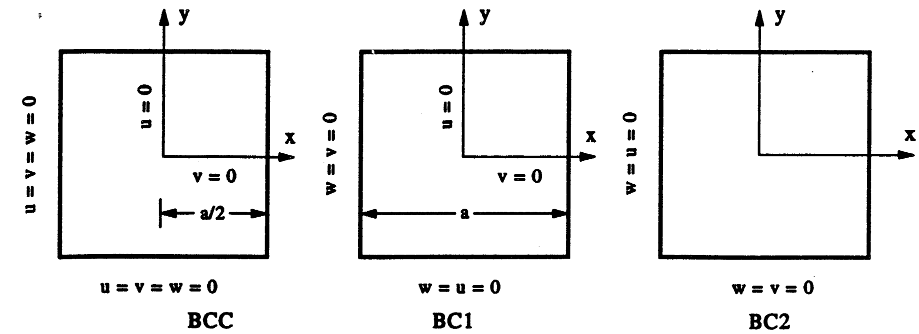

Fig. 4. Boundary conditions.

In the following some comparisons between the results obtained using the full Green–Lagrange strain tensor and its reduction by the Von Kármán assumptions are reported.

6. NUMERICAL RESULTS

In this section the formulation previously developed is used for the linear and nonlinear analysis of beams and rectangular plates, to demonstrate the efficiency and the validity of the proposed three-dimensional element. Table 1 contains a list of the material properties considered here. Figure 4 contains a list of the boundary conditions considered in this section.

6.1. *Transverse deflections*

6.1.1. *Clamped isotropic plate.* Consider a square clamped isotropic plate (BCC boundary conditions) of side $a = 1000$ mm, thickness $h = 2$ mm, and subjected to a uniformly transverse load $p = \lambda p_0$ ($p_0 = 1 \times 10^{-4}\,\mathrm{N\,mm^{-2}}$). The material is isotropic (material I). Owing to the symmetry only a quarter of the plate was analyzed by a $2 \times 2 \times 1$ mesh of 3DLW elements and the results are reported in Fig. 5, as a function of the load parameter. Comparisons are made with the analogous results obtained using the two-dimensional Generalized Laminated Plate Theory (2D-GLPT) [8, 15], where the boundary conditions were the following:

$$u_0 = v_0 = w_0 = \psi_x = \psi_y = 0$$

$$\text{at} \quad x = a/2 \quad \text{and} \quad y = a/2;$$

$$u_0 = \psi_x = 0 \quad \text{at } x = 0; \quad v_0 = \psi_y = 0 \quad \text{at } y = 0;$$

$\psi_x(x, y)$ and $\psi_y(x, y)$ being the rotations about the y and the x axes, respectively, and u_0, v_0, w_0 the middle-plane displacements. The central transverse deflections obtained by the proposed element compare well with those of Refs [8, 15].

In particular, it is possible to note that the two-dimensional solution was obtained using the Von Kármán approximations and it is the same of the 3DLW obtained using the full Green–Lagrange strain tensor.

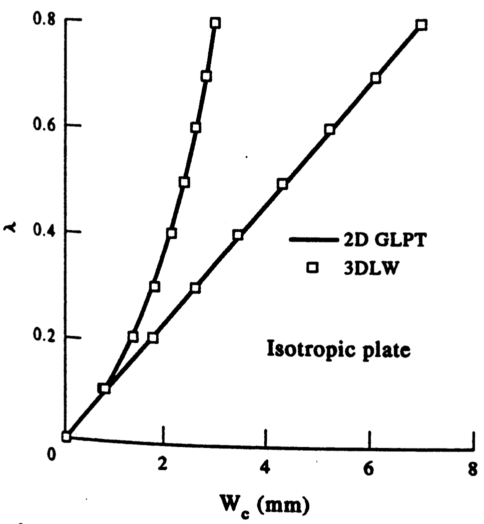

Fig. 5. Clamped square isotropic plate: linear and nonlinear central deflections.

6.1.2. *Cross-ply* [0°/90°] *simply supported plate.* A simply supported square cross-ply plate under uniformly transverse load is analyzed. The geometry is the same of case 6.1.1, and the load is expressed in terms of the load parameter λ using again $p_0 = 1 \times 10^{-4}\,\mathrm{N\,mm^{-2}}$.

The structure is composed of material II and the BC1 boundary conditions are used on one quarter of the plate with $2 \times 2 \times 2$ mesh of 3DLW. The comparisons, reported in Fig. 6 are made with the 2D-GLPT solution where the boundary conditions were:

$$v_0 = w_0 = \psi_y = 0 \quad \text{at } x = a/2;$$

$$u_0 = w_0 = \psi_x = 0 \quad \text{at } y = a/2;$$

$$u_0 = \psi_x = 0 \quad \text{at } x = 0;$$

$$v_0 = \psi_y = 0 \quad \text{at } y = 0.$$

Note that the use of the 3DLW (full Green–Lagrange) elements or the 2D-GLPT (Von Kármán) elements predicts practically identical values for the central transverse deflection.

6.1.3. *Simply supported angle-ply* [45°/−45°] *plate.* In order to make comparisons between the

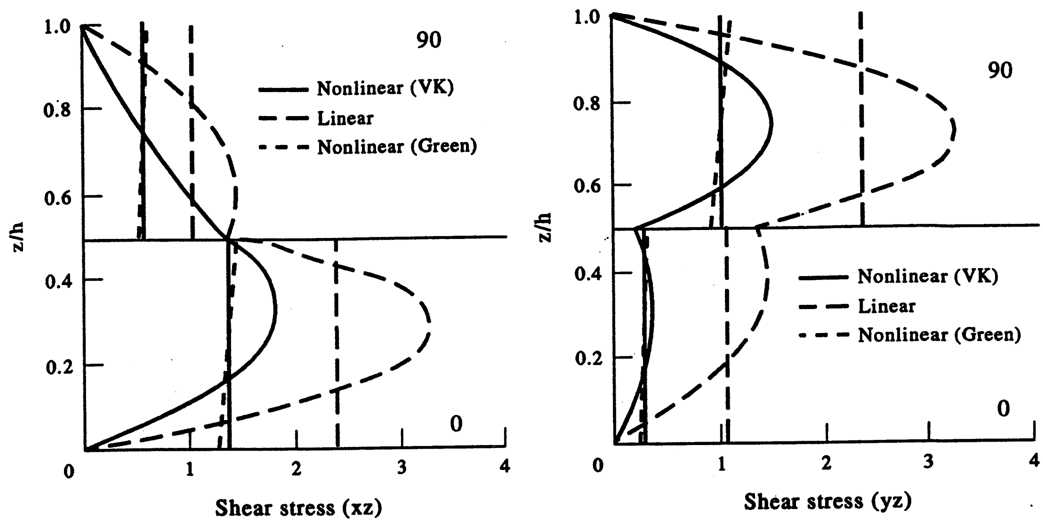

Fig. 10. Simply supported square cross-ply plate: through the thickness shear stress distribution (λ = 1.0).

6.2.2. *Stresses for a cross-ply* [0°/90°] *simply supported plate*. The plate of Section 6.1.2 is now considered to show the distribution of the normal and shear stresses through the thickness of the layers in the laminate. In particular the stresses are extrapolated to the nodal points. The shear stresses are adimensionalized by $(S_{ij}/p) \times 10^{-2}$ and the normal stresses by $(S_{ij}/p) \times 10^{-4}$. The normal stress S_{xx} is measured at the center of the plate ($x = y = 0$), while the S_{xz} stress is measured at $x = a/2$; $y = 0$ and the S_{yz} is measured at $x = 0$; $y = a/2$. The results are shown in Figs 9 and 10. In all the cases the nonlinear results are smaller than the linear ones.

For the shear stresses, the Von Kármán and the full Green–Lagrange nonlinear results obtained from constitutive equations are reported along with the quadratic shear stresses for equilibrium. It is easy to note that, when the full Green–Lagrange strain tensor is adopted, the presence of the derivatives of the u and v displacements with respect to the x and y coordinates, produces a linear variation of the shear stresses through the thickness of each layer. Instead, using the Von Kármán approximations these stresses are layer-wise constant. In any case the difference between the two results is very small. Then, the constant distribution of the shear stresses is used to be able to use the method proposed in Ref. [19] and obtain their parabolic distribution through the thickness.

6.3. *Beam ply drop-off problem*

To show the capability of the proposed element, an example of a cantilever beam with or without ply drop-off has been analyzed (Fig. 11). The ply drop-off is an important problem in the structures made of composite materials. The middle-surface is at different locations through the thickness in the thick and

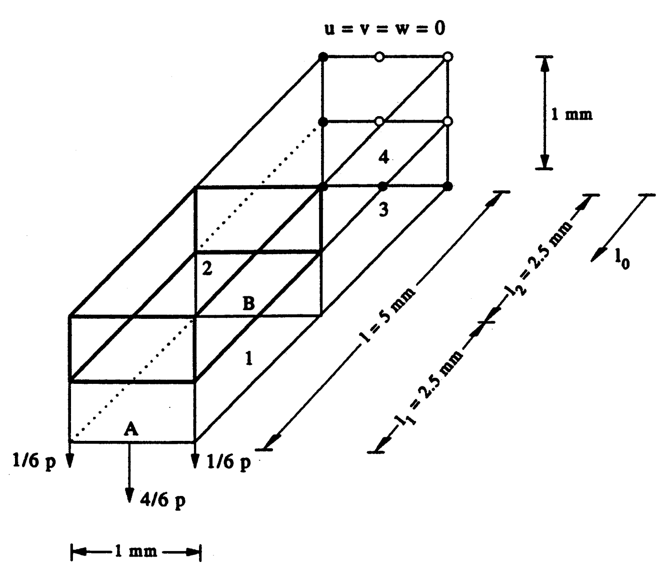

Fig. 11. Cantilever beam with ply drop-off: scheme and labels.

in the thin part of the beam. Thus, obtaining an exact solution or a finite element approximated solution for these irregular structures is a major problem. The use of the 3DLW elements overcomes this problem because, in comparison to the two-dimensional plate analysis, the position of the middle surface is irrelevant for the use of this element.

We start considering a beam without ply drop-off to check the results obtained using the proposed element by comparison between the analytical and the finite element solutions. The cantilever beam, made in material I (isotropic), is subjected to a compressive load $P = 100$ N applied in the transverse direction. In the linear case the Timoshenko beam theory was used to obtain the analytical solution [14]. The maximum deflection obtained analytically is equal to 2.5780 mm, while the finite element approximated solution is equal to 2.5336 mm. The nonlinear maximum deflection obtained with the 3DLW elements is equal to 1.8463 mm, showing that the nonlinearities produce a reduction of the deflections.

To model the ply drop-off beam, one element (number 2) was removed, as displayed in Fig. 11. Again the Timoshenko results are compared with the finite element ones. The analytical maximum deflection is equal to 4.8045 mm, while the finite element result is equal to 5.0455 mm. It can be noted that the 3DLW result is larger than the analytical solution. This is because the analytical solution assumes the two middle surfaces coincident, which is not the case in this example. With the 3DLW element we are also able to obtain the nonlinear maximum deflection, which is equal to 2.2006 mm showing a strong reduction with respect to the linear solution.

7. CONCLUSIONS

A previously developed element [11] has been extended for the geometrically nonlinear analysis of composite laminated plates. Furthermore, the incompressibility condition is imposed by a new method that preserves the symmetry of the stiffness matrix. Both the full Green–Lagrange strains and the Von Kármán strains have been considered. Post-computation of interlaminar stresses has been developed in terms of second Piola–Kirchhoff stresses and Von Kármán strains along the lines of the procedure presented in Refs [8, 13] for linear analysis. The procedure can be used only with Von Kármán strains and fails if Green–Lagrange strains are used. The element has been validated by comparisons with results from the literature and its versatility has been shown by modeling a ply drop-off problem.

Acknowledgements—The first author would like to acknowledge the financial support of the Italian Ministry of the University (Ph.D. courses). The first author also wishes to express his deep gratitude to his advisors, Professor Domenico Bruno and Giuseppe Spadea, for their inv... encouragement during this study.

REFERENCES

1. H. GangaRao and E. J. Barbero, *Utilization of ... posites in Construction. Encyclopedia on Comp...* Vol. 6, pp. 173–187. VCH (1991).
2. E. Reissner, The effect of transverse shear deform... on the bending of elastic plates. *J. appl. Mech.* **12**, A... (1945).
3. E. Reissner, Small bending and stretching of sandw... type shell. NACA-TN-1832 (1949).
4. R. D. Mindlin, Influence of rotatory inertia and sh... on flexural motions of isotropic elastic plates. *J. ... Mech.* **18**, 31 (1951).
5. J. N. Reddy, Exact solutions of moderately thick la... nated shells. *J. Engng Mech. Div. ASCE* **110**, 794 (198...
6. J. N. Reddy, On the generalization of displaceme... based laminate theories. *Appl. Mech. Rev.* **42**(... S213–S222 (1989).
7. J. N. Reddy, A generalization of two dimensio... theories of laminated plates. *Commun. appl. num... Meth.* **3**, 113–180 (1987).
8. E. J. Barbero, On a generalized laminate plate theo... with application to bending, vibration and delaminatio... buckling in composite laminates. Ph.D. Dissertatio... Virginia Polytechnic Institute and State Universit... Blacksburg, VA (1989).
9. S. Srinivas, Refined analysis of composite laminates. *J. Sound Vibr.* **30**, 495–507 (1973).
10. R. L. Hirichsen and A. N. Palazzotto, The nonlinea... finite element analysis of thick composite plates using a cubic spline function. *AIAA J.* **24**, 1836–1842 (1986).
11. E. J. Barbero, A 3D finite element for laminate... composites with 2D kinematic constraints. *Compu... Struct.* **45**(2), 263–271 (1992).
12. S. Ahmad, B. M. Irons and O. C. Zienkiewicz, Analysis of thick and thin shell structures by curved finite elements. *Int. J. numer. Meth. Engng* **2**, 419–451 (1970).
13. E. J. Barbero and R. Zinno, Analysis of laminated composite plates with three-dimensional layer-wise constant-shear elements. *Int. J. Engng Anal. Des.* **1**, 189–214 (1994).
14. R. Zinno and E. J. Barbero, A three-dimensional layer-wise constant shear element for general anisotropic shell-type structures. *Int. J. numer. Meth. Engng* **37**, 2445–2470 (1994).
15. E. J. Barbero and J. N. Reddy, Non linear analysis of composite laminates using a generalized laminated plate theory. *AIAA J.* **28**(11) (1990).
16. G. Porco, G. Spadea and R. Zinno, A geometrically nonlinear analysis of laminated composite plates using a shear deformation theory. *Atti Acc. Lincei rend. fis.* **LXXXIII**(8), 159–176 (1989).
17. L. E. Malvern *Introduction to the Mechanics of a Continuous Medium*. Prentice Hall, Englewood Cliffs, NJ (1969).
18. K. J. Bathe, *Finite Element Procedures in Engineering Analysis*. Prentice Hall, Englewood Cliffs, NJ (1982).
19. R. A. Chaudhuri, An equilibrium method for the prediction of transverse shear stresses in a thick laminated plate. *Comput. Struct.* **23**, 139–146 (1986).
20. R. D. Cook, *Concepts and Applications of Finite Element Analysis*, 2nd Edn. Wiley, New York (1974).
21. R. M. Jones, *Mechanics of Composite Materials*. Hemisphere, New York (1975).
22. J. N. Reddy, *Introduction to the Finite Element Method*. 2nd Edn. McGraw Hill, New York (1993).